Nonlinear effects in conductance histograms of atomic-scale metallic contacts

A. García-Martín,[1] M. del Valle,[1] J. J. Sáenz,[1] J. L. Costa-Krämer,[2] and P. A. Serena[3]
[1]*Departamento de Física de la Materia Condensada, Universidad Autónoma de Madrid, Cantoblanco, 28049 Madrid, Spain*
[2]*Instituto de Microelectrónica de Madrid, Consejo Superior de Investigaciones Científicas, Isaac Newton 8, PTM, 28760 Tres Cantos, Madrid, Spain*
[3]*Instituto de Ciencia de Materiales de Madrid, Consejo Superior de Investigaciones Científicas, Cantoblanco, 28049 Madrid, Spain*
(Received 25 February 2000)

General properties of conductance histograms of atomic-scale metallic contacts are discussed. Nonlinear effects are included assuming a quasiadiabatic representation for electron transport. Histograms of conductance and histograms of differential conductance markedly differ when increasing the bias voltage. Averaging over different nanowire breakage paths at high bias rapidly smears out the peaks in I/V histograms, while it leads to new peaks at half integer values in dI/dV histograms. Recent experimental results on the histograms evolution with the applied bias are discussed.

I. INTRODUCTION

During the last decade, nanotechnology has become an essential topic where multiple scientific disciplines meet, being a key for future technological developments. A fundamental branch of nanotechnology concerns the study of electronic transport through mesoscopic and low dimensional systems.[1,2] The practical realization of such systems has been based on devices working at low temperatures, where an electronic current flows in a two-dimensional electron gas (2DEG) under a bias voltage. With this background, it has been possible to develop two-dimensional (2D) constrictions, quantum dots, cavities presenting chaotic features, etc. In particular, the study of electronic propagation through small constrictions has received attention in order to test basic physical ideas and propose new electronic devices.

Although 2DEG based devices have been for a long time suitable to analyze basic aspects of mesoscopic systems, a great effort has been made to use metallic contacts of nanometric size, metallic nanowires, to study the basic features of quantum transport, opening a path to use them as interconnects among active elements in integrated systems.[3] The characteristic small dimensions of such contacts (only a few times the Fermi length λ_F) make them appropriate to study phenomena such as ballistic transport or conductance quantization (CQ). CQ is an appealing phenomenon which reveals the quantum nature of electron transport when only a few transversal modes (due to the electron spatial confinement) are populated. In this case, the measured conductance $G=I/V$ (where I is the current intensity and V the applied bias voltage across the constriction) is given, in the small bias limit, by the expression $G=N2e^2/h=NG_0$, where G_0 is the conductance quantum, N reflects the number of allowed propagating modes, e is the electron charge, and h is the Planck constant.[4] Although CQ was confirmed in 2DEG devices,[5,6] the study of such phenomenon in metallic nanocontacts has attracted special attention because it should be noticeable even at room temperature due to the relatively large energy separation between transversal modes.

Nowadays, it is possible to create metallic nanocontacts, with minimal sections formed by a few atoms, using techniques based on either the scanning tunneling microscopy (STM),[7–10] or the mechanically controllable break junction (MCBJ) method.[11,12] Using both experimental approaches, based on piezo-controlled motions, it is feasible to stabilize the contact structure at atomic level during a long time, keeping a constant electron current. The presence of conductance steps of the order of G_0 when the nanocontact section changes has been interpreted as a CQ signature.

The electrical characterization of these low dimensional systems is a topic of great interest and several experiments have measured current-voltage (IV) characteristics at different conductance values.[8,10,13–15] In general, the measured IV curves show a characteristic nonlinear behavior more strongly marked in situations where only a few conductance channels are involved.[8,10] These nonlinear features can be negligible when the nanocontact is formed over a substrate.[15] A remarkable feature observed in the free-standing metallic nanocontact IV curves is that the nonlinear component increases with a power law $I\sim V^q$ where the exponent q ranges between 2 and 3.[10] This behavior differs from that observed in microfabricated 2DEG constrictions where the strong nonlinear behavior is seen as a change of slope in the IV curve.[16,17] These changes in the slope also give rise to $G_0/2$ steps in the differential conductance $g=\delta I/\delta V$ when the nanocontact section A varies.[18] These new plateaus in $g(A)$ are explained in terms of a model that assumes the applied bias voltage drops symmetrically with respect to the nanocontact middle point.[19,20] A similar behavior is found in three-dimensional constrictions[21,22] although, in this case, the IV curves show an additional dependence on the 3D induced degeneracy of the transversal modes. The predicted behavior for the curve $g(V)$ in 3D nanocontacts[21] has not been experimentally observed. Several explanations have been proposed in order to explain this disagreement, ranging from the existence of Coulomb blockade[23] to the presence of a nonnegligible tunnel current contribution which depends on the nanocontact geometry[22] or to the presence of impurities in the contact region.[24]

In a different context, the IV traces appearing in metallic nanocontacts in the superconductor regime have been used to estimate the number of channels involved in the electron

transport when conductances close to G_0 are measured.[25] The obtained experimental results seem to support the idea that the chemical valence determines the number of allowed conducting channels in single-atom contacts,[26] although the presence of geometrical effects should be accounted for.[27]

Not only the electrical characterization of metallic nanocontacts and nanowires has been the subject of study, but the CQ phenomenon itself in such systems has been extensively analyzed. A tool to get insight on CQ lies in the elaboration of histograms of conductance. Due to the inherent nonreproducibility of similar atomic structures during nanocontact breakage experiments, some statistical tool is needed. Counting conductance occurrences for different retraction experiments and building a histogram of conductance values is one, perhaps the simplest, of such tools.[12,28] Although there is a vivid debate about the origin and meaning of such conductance histograms,[25,27,29] the evaluation and construction of histograms has become a standard tool in the study of the conductance quantization phenomenon under different situations. Conductance histograms obtained for nanocontacts formed between two macroscopic metal wires demonstrated the strength of the CQ phenomenon[30] and its independence on the experimental setup. Different kinds of experiments using conductance histograms have been presented in order to analyze the CQ dependence on different external parameters such as chemical environment,[31] temperature,[32] magnetic field,[33–35] retraction speed in STM-like nanowire breaking experiments,[33] etc.

Following the same experimental methodology, a recent work[36,37] shows a strong dependence of the histogram peaks on the applied voltage. With increasing bias voltage the peak height decreases and finally disappears at some critical voltage V_c. In particular the peak corresponding to $G=G_0$ disappears at $V_c \approx 1.9$ V at room temperature whereas $V_c \approx 2.2$ V at liquid-nitrogen temperature. This experimental result was interpreted in terms of electromigration induced for huge current densities in the nanocontact. Although this explanation presents a reasonable physical framework it neglects the nonlinearity in the *IV* curve which can play an important role at such high voltages. A very interesting question arises when observing the conductance histograms under applied voltage. In principle, the nonlinear term appearing in *IV* measurements should shift the histogram peaks towards higher G values but experimental findings do not reveal any noticeable shift. There are even results indicating that the shift is towards lower G values for increasing applied voltage.[38] The aim of the present work is to explain the observed evolution of conductance histograms as consequence of the nonlinear behavior of the *IV* characteristic curve, thus offering a contribution which coexists with the diffusion and electromigration ones.

The structure of the paper is as follows: in Sec. II we present the model for a 3D metallic contact and the method to determine the conductance histograms including finite bias voltages; in Sec. III we present calculated histograms and analyze the voltage influence and its dependence on the voltage drop across the nanowire; finally, in Sec. IV the main conclusions are summarized.

II. THEORETICAL MODEL

A. Nonlinear conductances

A deep insight in the physics of quantum electronic transport through small contacts is obtained from Landauer's scattering approach to electrical conductance.[4] An atomic-scale metallic contact can be considered as a small connecting nanowire between two three-dimensional electron gases. The quantization of the transversal momentum of the electrons defines different subbands or channels, each having an associated transmission probability T_n to go from the subband n in one reservoir to the other.

In a metallic 3D constriction, the electrons are confined in the transversal directions whereas transport occurs only along the other one, let us call it the z direction. Therefore each channel has a momentum k_z in the transport direction, and the dispersion relation for each channel in the reservoirs results in $\epsilon=\epsilon(n,k_z)=E_z(k_z)+\epsilon_n$, where ϵ_n is the characteristic transversal energy of the channel n. Thus the number of channels N in each reservoir is given by the maximum value n satisfying $\epsilon_n<E_F$. The contribution to the current of a given channel in the left reservoir for a differential energy interval $d\epsilon$ is given by the product of the electric charge e, the group velocity $(1/\hbar)d\epsilon/dk_z$, the density of states along the wire $\rho_n(\epsilon)d\epsilon$, and the transmission probability for an electron to go from the channel n in the left reservoir to the right reservoir,

$$dI_n^{l\to r}=e\frac{d\epsilon}{\hbar dk_z}\rho_n(\epsilon)d\epsilon T_n(\epsilon,V). \tag{1}$$

A similar expression is obtained for electrons in the right reservoir *arriving to* the channel n in the left one,

$$dI_n^{r\to l}=e\frac{d\epsilon}{\hbar dk_z}\rho_n(\epsilon)d\epsilon T_n(\epsilon-eV,V), \tag{2}$$

where applied bias voltage shifts the energy at which the transmission probability is evaluated. After including the spin degeneracy, the density of states is given by $\rho_n(\epsilon)=(1/\pi)dk_z/d\epsilon$. The total current is therefore given by the summation over all the channels and integration over the energy spectrum

$$I=\frac{2e}{h}\int_{E_F-eV}^{E_F}\sum_n^{N'(\epsilon)} T_n(\epsilon,V)d\epsilon, \tag{3}$$

where $N'(\epsilon)$ gives the number of channels satisfying $\epsilon_n<\epsilon$. Here we have used the fact that the Fermi-Dirac distribution (implicit in the density of states accounting for temperature effects) at room temperature is well approximated by the step function.

For finite bias V, we must distinguish between the conductance G and the differential conductance g. The conductance G is defined as the inverse of the resistance $G\equiv I/V$ whereas the differential conductance g is defined as $g\equiv dI/\mathrm{d}V$,

$$g=\frac{\partial}{\partial(eV)}\int_{E_F-eV}^{E_F}\tilde{g}(\epsilon)d\epsilon, \tag{4}$$

$$\tilde{g}(\epsilon,V)\equiv G_0\sum_n^{N'(\epsilon)} T_n(\epsilon,V). \tag{5}$$

Following previous approaches[21,39,40] we assume that, in general, the voltage drops a fraction βV between the left

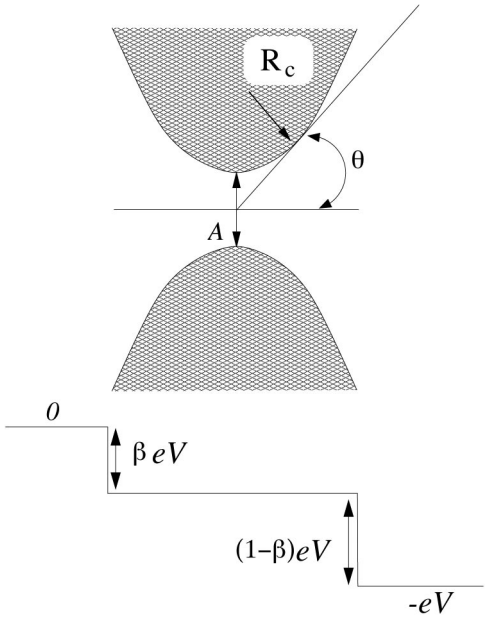

FIG. 1. Schematic representation of the contact model. The potential profile at a bias V is also sketched.

reservoir and the contact and $(1-\beta)V$ between the constriction and the right reservoir, while the potential remains constant inside the constriction itself[41] (β accounts for any asymmetry of the potential drop). $\beta=1/2$ implies a symmetric drop while $\beta=1$ implies a perfect drop betweeen the negative electrode and the contact (see the scheme in Fig. 1). The actual potential drop along atomic-size constrictions is a difficult problem that has been recently addressed within self-consistent tight-binding[42] and *ab initio* local-density[43] calculations. For gold contacts and small bias ($V\lesssim 0.5$ V), the potential drop was found to be approximatelly symmetric ($\beta\approx 1/2$).[43] Interestingly, as a consequence of asymmetries in the local-density of states, the potential drop at higher bias can be highly asymmetric ($\beta\approx 1$) even for geometrically symmetric contacts.

Under the assumption of quasiadiabatic transport,[18,21,39,40] $\tilde{g}(\epsilon,V)$ only depends on the energy difference between the incoming electrons and the bottom of the electrostatic potential, i.e., $\tilde{g}(\epsilon,V)\approx\tilde{g}(\epsilon+\beta\ \text{eV})$. Thus we obtain for the conductance

$$G(V)=\frac{I}{V}\approx\frac{1}{eV}\int_{E_F-(1-\beta)eV}^{E_F+\beta eV}\tilde{g}(\epsilon)d\epsilon. \tag{6}$$

Under the same approach the differential conductance g is then given by the weighted average of two zero-voltage conductances at different effective Fermi energies:[44]

$$g(V)\approx\beta\tilde{g}[E_F+\beta\ \ eV]+(1-\beta)\tilde{g}(E_F-(1-\beta)\ \ eV). \tag{7}$$

As expected, in the limit of zero bias, Eqs. (6) and (7) recover Landauer's formula

$$G(V\to 0)=g(V\to 0)=\tilde{g}(E_F)=\frac{2e^2}{h}\sum_n^{N(E_F)}T_n(E_F). \tag{8}$$

We should emphasize that Eqs. (6) and (7) provide a simple approach to an otherwise extremelly complex problem. The energy dependence of transmission probabilities $T_n(\epsilon,V)$ in actual contacts depend on the local chemistry and geometry around the contact and may change with the applied bias V. This bias dependence, which for gold contacts is important only for high bias ($V\gtrsim 2$ V),[43] should then be taken into account in any detailed quantitative analysis of the experimental results.

B. Saddle-point contact model

In order to calculate transmission coefficients, we consider a simple saddle-point contact (SPC) model, originally introduced by Büttiker,[45] and used to describe electronic transport in two-dimensional systems.[39] The SPC model was shown to be very useful in the analysis of different transport properties in three-dimensional constrictions.[27,46] In this model the constriction geometry connecting the two reservoirs is given by the equipotential surface $V(x,y,z)=\epsilon$, where ϵ is the electron kinetic energy at the narrowest part of the constriction. $V(x,y,z)$ can be written as

$$V(x,y,z)=\epsilon\frac{\pi}{A}\left(\frac{1}{\eta}x^2+\eta y^2-\sqrt{A/\pi}\,\frac{1}{R_c}z^2\right). \tag{9}$$

Electronic transport takes place along the z direction, whereas electrons are confined in the transversal directions by parabolic potentials. The constriction geometry as sketched in Fig. 1 looks like a parabolic geometry with ''elliptical'' cross section. A is the area of the narrowest section, R_c is the radius of curvature and η describes the degree of anisotropy of the elliptical cross section. We may also define in this case an opening angle θ,[47] given by

$$\tan^2(\theta)\equiv(\sqrt{A/\pi})/R_c\,. \tag{10}$$

The transmission probability of the n,m channel can be calculated exactly in closed form and takes the simple form

$$T_{nm}(\epsilon)=\left\{1+\exp\left(\frac{-2\pi[\sqrt{\pi(A/\lambda_F^2)(\epsilon/E_F)}-\epsilon_{nm}]}{\tan(\theta)}\right)\right\}^{-1} \tag{11}$$

with $\epsilon_{nm}=(n+1/2)/\sqrt{\eta}+\sqrt{\eta}(m+1/2)$. We take a constant value $\eta=0.668$ in order to break the channel degeneracy (this is known to be a good approximation for gold contacts[27]). The qualitative results will not depend on the exact η value, however.

III. RESULTS AND DISCUSSION

A. Conductance versus differential conductance at finite bias

Although for very small bias G and g are exactly the same quantities, there are strong differences at higher bias. In order to emphasize these differences in Fig. 2 we have plotted the current I and both g and G versus the applied bias V for a contact with fixed opening angle $\theta=10°$ at different cross sections. Figure 2(b) shows the characteristic evolution of g versus V for $\beta=1/2$. The evolution from quantum plateaus at integer multiples of G_0 towards half integer values can be clearly seen. Nonlinear effects change in a noticeable way

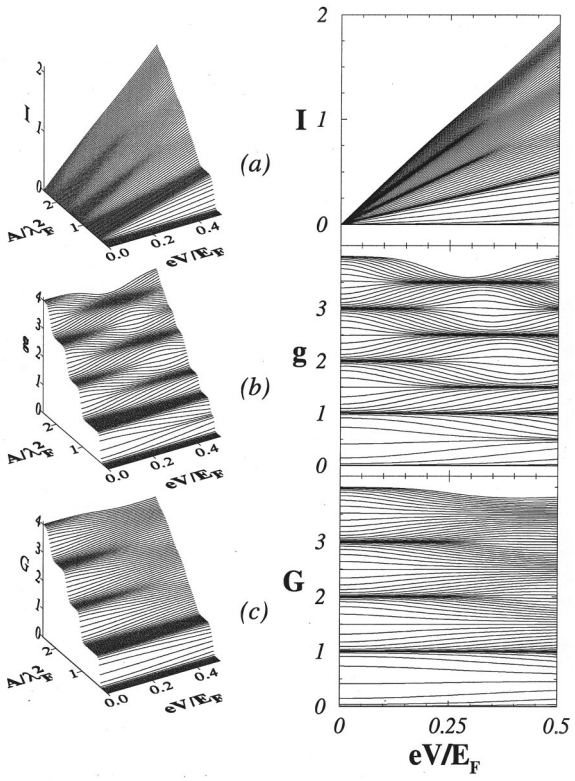

FIG. 2. Current intensity I (a), differential conductance $g=dI/dV$ (b), and conductance $G=I/V$ (c) (both in units of G_0), versus voltage V for different sections A of the three-dimensional constriction depicted in Fig. 1 with $\theta=10°$ and $\beta=1/2$.

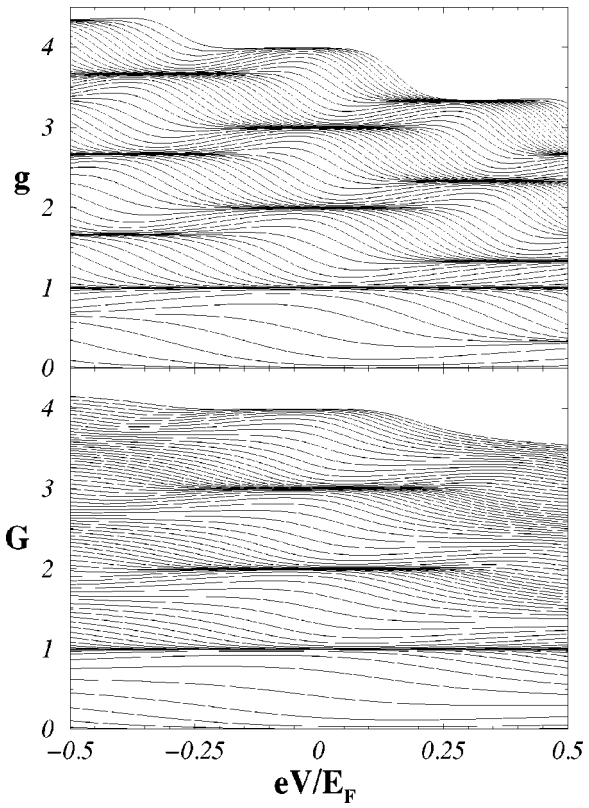

FIG. 3. Differential conductance g and conductance G in units of G_0 versus V for different sections A of the three-dimensional constriction shown in Fig. 1 with $\theta=10°$ and $\beta=1/3$.

$g(V)$ for voltages larger than $0.15E_F/e$ (i.e., $0.8V$ for gold). In contrast, the behavior of the conductance G [see Fig. 2(c)] does not show this evolution to noninteger multiples of G_0 and the quantum plateaus gradually disappear.

The effect of a possible asymmetry in the potential drop across the constriction is illustrated in Fig. 3 where we have plotted both g and G versus V for $\beta=1/3$. At very small bias, the asymmetry induces a linear dependence of the conductance with V (except very close to integer multiples of the conductance quantum). At higher bias, the quantum plateaus in g evolve gradually towards new plateaus at $(n+1/3)G_0$ $(V>0)$ and $(n+2/3)G_0$ $(V<0)$ following Eq. (7). As it was shown for $\beta=1/2$ the conductance G does not present any plateau at noninteger G/G_0 values in the high-voltage regime.

B. Conductance histograms

In metallic contacts, the behavior of the conductance with elongation is a stepwise curve. In general, the position of the steps and the conductance plateau value change from one experiment to another. However, and notably for noble metals such as gold, copper, and silver, plateaus tend to appear close but slightly below integer values of G_0. This is evidenced in the histograms as peaks near, but slightly below, integer values of G_0. This has been explained in terms of structural disorder making transmission coefficients deviate from perfect transmission.[48,49]

A detailed theoretical description of the mechanical and electrical properties of the contact during elongation is a very difficult task.[50] A qualitative picture, however, can be obtained from the model system discussed above, together with an *effective elongation path*:[27] Let us assume that, for small contacts, the cross section A follows an almost exponential dependence with the displacement d. The actual evolution of the contact geometry with elongation does not correspond to a constant angle θ but, in general, would be a nontrivial function $\theta(A)$ which will change from one contact to another.[51] In a typical experiment the conductance versus elongation curves present conductance plateaus which, in general, do not correspond to exact integer multiples of G_0. Repetitive cycles of elongation-retraction processes usually give similar stepped curves but with plateaus at different conductance values, i.e., the stepped conductance curve change from one experiment to another. This is schematically illustrated in Fig. 4 where dashed line and thin continuous line would represent two different single experimental realizations in a typical elongation-contraction process). The effective elongation path would correspond to the experimental average of many individual G vs d curves (thick line in Fig. 4). This effective path can be estimated as follows: within the SPC model, the radius of curvature of the contact R_C/λ_F should be of the order of or larger than 1 in order to have no unphysical tunneling contributions to the conductance (actually, in metallic contacts R_C should be larger than an atomic radius $\approx\lambda_F$). For simplicity, we consider an effective path at constant $R_C=2\lambda_F$, being the effective path $\theta(A)$ given by Eq. (10) (the results will not depend—qualitatively—on the exact dependence of A on d). Assuming that the contact can take any section along this path we obtain the conductance histogram shown in Fig. 5(a) (notice

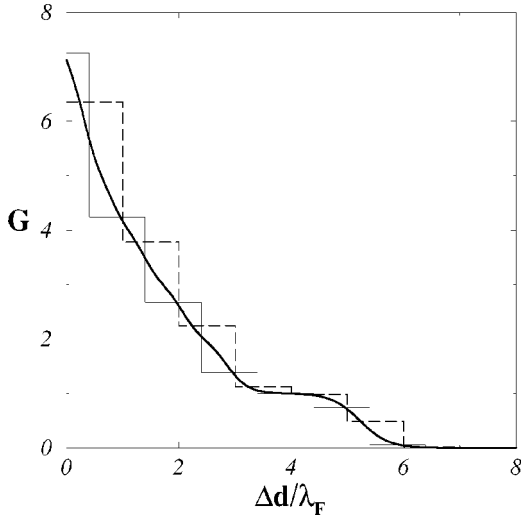

FIG. 4. Conductance in units of G_0 as a function of the contact elongation Δd for an effective elongation path with constant $R_C = 2\lambda_F$ and zero bias (see text). The dashed line and thin continuous line would represent two different single experimental realizations in a typical elongation-contraction process. The thick line represents the average conductance along the effective path.

that at zero bias the histograms of G and g are exactly the same). Despite the simplicity of the model, the obtained histogram at zero bias is very similar to the experimental histograms for Au contacts. Although experimental conductance histograms present a rich structure (peaks asymmetry, peaks displacements towards lower values, etc.) the important point in this study will concern the height of the histogram peaks. The relative peaks height obtained with our effective elongation path approximation is rather similar to that found experimentally and thus represents a good starting point to include voltage effects. Most of the experimental studies are concerned with histograms at low biases. Recently, Yasuda and Sakai[36,37] have obtained a strong dependence of the conductance (G) histogram peaks with the applied voltage. As we are going to show, our simple model can qualitatively explain their experimental observations.

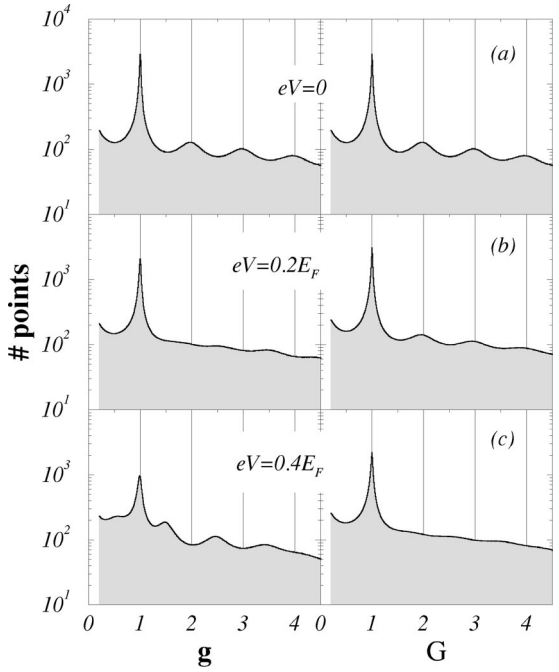

FIG. 5. Differential conductance g and conductance G (in units of G_0) histograms [$H(g)$ and $H(G)$] obtained from the effective elongation path sketched in Fig. 4 at different bias, (a) $eV=0$, (b) $0.2E_F$, (c) $0.4E_F$. The potential drop is assumed to be symmetric ($\beta=1/2$).

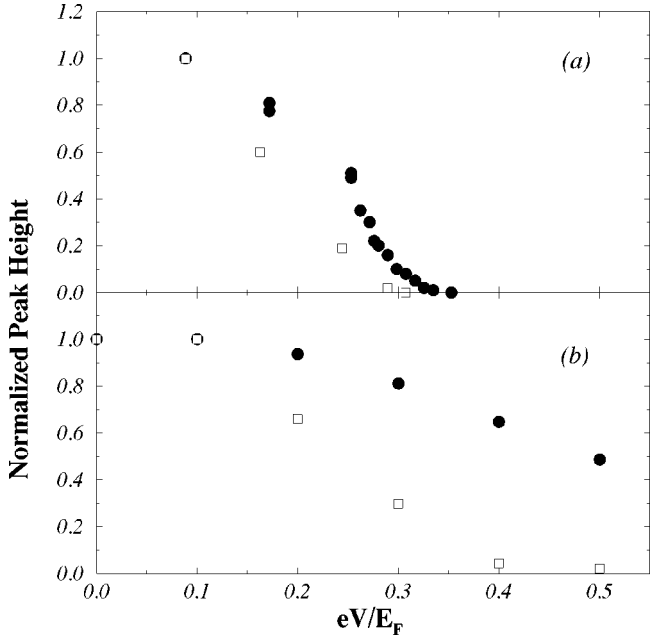

FIG. 6. Experimental (a) and theoretical (b) bias dependence of the normalized peak height for the first $1G_0$ peak (closed circles) and for the second $2G_0$ peak (open circles) of the conductance histograms $H(G)$. The peak heights are normalized at their values at $V=0.1E_F$.

The behavior of g and G histograms [$H(g)$ and $H(G)$] changes completely for finite bias [Figs. 5(b) and 5(c)]. As V increases, the peaks at integer multiples of G_0 gradually disappear, except the first one which remains at high voltages. In $H(g)$ new peaks at half integer values can clearly be seen for $V > \approx 0.3E_F$. In contrast, $H(G)$ do not show traces of conductance quantization above $\approx 0.4E_F$ (for gold contacts, $E_F \approx 5.5$ V). Except for the behavior of the first peak at $1G_0$, the agreement with the experimental results of G histograms of Yasuda and Sakai is remarkable. In order to make the comparison more quantitative, following Ref. 37, in Fig. 6 we have plotted both the experimental (a) and theoretical (b) heights of the first and second peak in $H(G)$ versus the applied bias V [the peak height is measured with respect to the background in $H(G)$]. The qualitative agreement between theory and experiment suggests that the dissapearance of peaks at G larger than $1G_0$ may be partially explained in terms of nonlinear effects in the ballistic conductance. The faster decrease in the experimental peak heights together with the absence of the first peak at high bias could indicate that effects like atomic diffusion and electromigration by current-induced forces[52,53] may also play an important role. These effects would lead to fluctuations of the conductance (contact cross section) with time. If the experimental time window used to measure a conductance value averages it between different cross sections the peak structure of the histogram would disappear.[54] As a matter of fact, the experi-

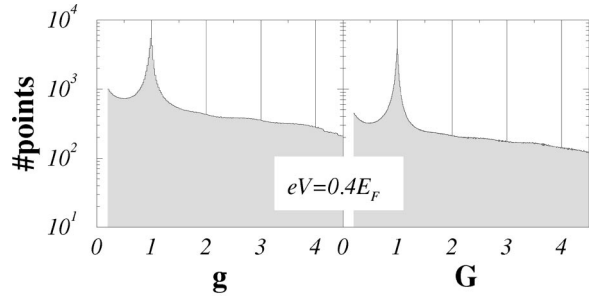

FIG. 7. Differential conductance g and conductance G (in units of G_0) histograms [$H(g)$ and $H(G)$] obtained from the effective elongation path sketched in Fig. 4 at $V=0.4E_F$, after averaging between $\beta=0$ and $\beta=1$.

mental behavior of the height of the first peak changes above ≈ 1.5 V (see Fig. 4 in Ref. 37), which could indicate a bias threshold for voltage induced electromigration. Therefore, histogram evolution under increasing applied bias has two different regimes: a first one governed by nonlinear effects and a second one where electromigration plays a more important role. Each regime should show its own rate of peak height decrease as might be extracted from the experimental data. It would be interesting to study the peak height behavior as a function of temperature (the only available results correspond to room temperature). Since electromigration is also a thermal activated process, we expect a shift of the threshold bias towards higher values. This trend with temperature in experimental data can be seen when inspecting Fig. 4 of Ref. 36 where the rate at which conductance histogram peaks disappear strongly depends on the temperature. In particular, we expect that the experimental curve shown in Fig. 6(a) will change at lower temperatures towards the theoretical predictions shown in Fig. 6(b).

We would like to point out that there is another factor that may prevent the observation of peaks at high bias, even in $H(g)$. Let us suppose that for some reason (particular geometrical arrangements, chemical environment, etc.) the potential drop along the nanocontact is different for each experimental realization. In that case, the resulting experimental histogram would be an average of histograms having different β factors. In Fig. 7 we have plotted that histogram assuming a uniform distribution of β values between 0 and 1. As it can be seen, the final histogram is very similar to $H(G)$, i.e., it does not show any peak other than that corresponding to the first quantum.

IV. CONCLUSIONS

In this work we have constructed theoretical histograms, of both the total (G) and differential (g) conductances, for nanometric-sized nanocontacts involving only a few propagating modes. Nonlinear effects induced by the bias voltage V applied between the two electrodes (electronic reservoirs) have been included assuming a quasiadiabatic representation for electron transport, obtaining explicit dependences for G and g on V. Histograms calculation involves basically one ingredient: the knowledge of the nanocontact geometry time evolution. We have used two approximations to describe this evolution during the metallic nanowire breakage experiments. On one hand, we have described the geometry of the contact using a saddle-point contact (SPC) model where the main geometrical features (minimum cross section and opening angle) are easily included. On the other hand, the nanowire dynamics has been averaged giving rise to an effective elongation path.

The main result is that histograms of conductance $H(G)$ and differential conductance $H(g)$ markedly differ for increasing applied voltages. The histogram $H(G)$ losses its peaked structure at voltages $\sim 0.2E_F$ whereas $H(g)$ keeps its structure up to higher voltages. This difference has to do essentially with the richest structure noticed by $g(V)$ in comparison to that found in $G(V)$. In this last case, the average over many different nanowire breakage paths rapidly smears out the peaked histogram. This evolution with V agrees with experimental observations, although some interpretations of such results were given in terms of electromigration enhanced diffusive processes in the nanocontact region. Here a different explanation is provided, based on nonlinear conductance effects that appear for increasing voltages. Our explanation does not exclude electromigration contributions at high voltages. In fact, experimental histograms reflect the existence of two voltage dependence regions with different peak disappearance rate. The histogram structure in the first voltage interval should be governed by the appearance of nonlinear effects on $G(V)$. Above a threshold voltage, the electromigration contribution washes out the peaked structure.

In order to clarify the actual origin for the histogram degradation at high voltages different kinds of experiments can be proposed. For instance, accumulate histograms for both G and g in order to see if the corresponding degradation rate with voltage differs or not. In the same fashion, interesting information could be gathered from controlled environment experiments, where surrounding substances (oil, glycerin, etc.) will hinder diffusive contributions.

ACKNOWLEDGMENTS

We acknowledge stimulating discussions with T. López-Ciudad and J. I. Pascual. This work has been partially supported by the Comunidad Autónoma de Madrid (Spain) through Project No. 07N/0024/1998, the Spanish DGESIC (MEC) through Project No. APC1998-0174, and the DGICyT (MEC) with Project No. PB98-0464.

[1] S. Datta, *Electronic Transport in Mesoscopic Systems* (Cambridge University Press, Cambridge, 1995).

[2] Y. Imry, *Introduction to Mesoscopic Physics* (Oxford University Press, Oxford, 1997).

[3] *Nanowires*, Vol. 340 *of NATO Advanced Study Institute*, Series E: Applied Sciences, edited by P. A. Serena and N. García (Kluwer, Dordrecht, 1997).

[4] R. Landauer, Z. Phys. B: Condens. Matter **68**, 217 (1987); J. Phys.: Condens. Matter **1**, 8099 (1989).

[5] D. A. Wharam, T. J. Thronton, R. Newbury, M. Pepper, H. Ahmed, J. E. F. Frost, D. G. Hasko, D. C. Peacock, D. A. Ritchie, and G. A. C. Jones, J. Phys. C **21**, L209 (1988).

[6] B. J. van Wees, H. van Houten, C. W. J. Beenakker, J. G. Williamson, L. P. Kouwenhoven, D. van der Marel, and C. T. Foxon, Phys. Rev. Lett. **60**, 848 (1988).
[7] L. Olesen, E. Laegsgaard, I. Stensgaard, F. Besenbacher, J. Schiotz, P. Stolze, K. W. Jacobsen, and J. K. Norskov, Phys. Rev. Lett. **72**, 2251 (1994).
[8] J. I. Pascual, J. Méndez, J. Gómez-Herrero, A. M. Baró, N. García, U. Landman, W. D. Luedtke, E. N. Bogacheck, and H.-P. Cheng, Science **267**, 1793 (1995).
[9] N. Agraït, G. Rubio, and S. Vieira, Phys. Rev. Lett. **74**, 3995 (1995).
[10] J. L. Costa-Krämer, N. García, P. García-Mochales, P. A. Serena, M. I. Marqués, and A. Correia, Phys. Rev. B **55**, 5416 (1997).
[11] C. J. Muller, J. M. van Ruitenbeek, and L. J. de Jongh, Phys. Rev. Lett. **69**, 140 (1992).
[12] J. M. Krans, J. M. van Ruitenbeek, V. V. Fisun, I. K. Yanson, and L. J. de Jongh, Nature (London) **375**, 767 (1995).
[13] V. V. Dremov and S. Yu. Shavopal, JETP Lett. **61**, 336 (1995) [Pis'ma Zh. Éksp. Teor. Fiz. **61**, 321 (1995)].
[14] B. Rodell, V. Korenivski, J. Costa, and K. V. Rao, Nanostruct. Mater. **7**, 229 (1996).
[15] A. Correia, J.L. Costa-Krämer, Y. W. Zhao, and N. García, Nanostruct. Mater. **12**, 1015 (1999).
[16] R. J. Brown, M. J. Kelly, M. Pepper, H. Ahmed, D. G. Hasko, D. C. Peacock, J. E. F. Frost, D. A. Ritchie, and G. A. C. Jones, J. Phys.: Condens. Matter **1**, 6285 (1989).
[17] L. P. Kouwenhoven, B. J. van Wees, C. J. P. M. Harmans, J. G. Williamson, H. van Houten, C. W. Beenakker, C. T. Foxon, and J. J. Harris, Phys. Rev. B **39**, 8040 (1989).
[18] L. I. Glazman and A. V. Khaetskii, Europhys. Lett. **9**, 263 (1989).
[19] N. K. Patel, L. Martín-Moreno, M. Pepper, R. Newbury, J. E. F. Frost, D. A. Ritchie, G. A. C. Jones, J. T. M. B. Janssen, J. Singleton, and J. A. A. J. Perenboom, J. Phys.: Condens. Matter **2**, 7247 (1990).
[20] N. K. Patel, J. T. Nicholls, L. Martín-Moreno, M. Pepper, J. E. F. Frost, D. A. Ritchie, and G. A. C. Jones, Phys. Rev. B **44**, 13 549 (1991).
[21] J. I. Pascual, J. A. Torres, and J. J. Sáenz, Phys. Rev. B **55**, R16 029 (1997).
[22] A. Garcia-Martín, T. Lopez-Ciudad, J. A. Torres, A. J. Caamaño, J. I. Pascual, and J. J. Sáenz, Ultramicroscopy **73**, 199 (1998).
[23] J. L. Costa-Krämer, N. García, M. Jonson, I. V. Krive, H. Olin, P. A. Serena, and R. I. Shekhter in *NanoScience and Technology*, Vol. 348 of *of NATO Advanced Study Institute*, Series E: Applied Sciences, edited by N. García, M. Nieto-Vesperinas, and H. Rohrer (Kluwer, Dordrecht, 1998), p. 1.
[24] K. Hansen, S. K. Nielsen, E. Laegsgaard, I. Stensgaard, and F. Besenbacher, Rev. Sci. Instrum. **71**, 1793 (2000).
[25] E. Scheer, P. Joyez, D. Esteve, C. Urbina, and M. H. Devoret, Phys. Rev. Lett. **78**, 3535 (1997).
[26] E. Scheer, N. Agraït, J. C. Cuevas, A. Levy-Yeyati, B. Ludolph, A. Martín-Rodero, G. Rubio-Bollinger, J. M. van Ruitenbeek, and C. Urbina, Nature (London) **394**, 154 (1998).
[27] T. López-Ciudad, A. García-Martín, A. J. Caamaño, and J. J. Sáenz, Surf. Sci. **440**, L887 (1999).
[28] L. Olesen, E. Laegsgaard, I. Stensgaard, F. Besenbacher, J. Schiøtz, P. Stoltze, K. W. Jacobsen, and J. K. Nørskov, Phys. Rev. Lett. **74**, 2147 (1995).
[29] A. I. Yanson and J. M. van Ruitenbeek, Phys. Rev. Lett. **79**, 2157 (1997).
[30] J. L. Costa-Krämer, N. García, P. García-Mochales, and P. A. Serena, Surf. Sci. **342**, L1144 (1995).
[31] C. Z. Li, H. Sha, and N. J. Tao, Phys. Rev. B **58**, 6775 (1998).
[32] B. B. Lewis, K. G. Vandervoort, and R. Foster, Solid State Commun. **109**, 525 (1999).
[33] J. L. Costa-Krämer, Phys. Rev. B **55**, R4875 (1997).
[34] H. Oshima and K. Miyano, Appl. Phys. Lett. **73**, 2203 (1998).
[35] T. Ono, Y. Ooka, H. Miyajima, and Y. Otani, Appl. Phys. Lett. **75**, 1622 (1999).
[36] H. Yasuda and A. Sakai, Phys. Rev. B **56**, 1069 (1997).
[37] K. Itakura, K. Yuki, S. Kurokawa, H. Yasuda, and A. Sakai, Phys. Rev. B **60**, 11 163 (1999).
[38] J. L. Costa-Krämer, N. García, P. García-Mochales, P. A. Serena, M. I. Marqués, and A. Correia, in Ref. 3, p. 171.
[39] L. Martín-Moreno, J. T. Nicholls, N. K. Patel, and M. Pepper, J. Phys.: Condens. Matter **4**, 1323 (1992).
[40] Hongqui Xu, Phys. Rev. B **47**, 15 630 (1993).
[41] P. L. Pernas, A. Martín-Rodero, and F. Flores, Phys. Rev. B **41**, 8553 (1990).
[42] T. N. Todorov, Philos. Mag. B **79**, 1577 (1999).
[43] M. Brandbyge, N. Kobayashi, and M. Tsukada, Phys. Rev. B **60**, 17 064 (1999).
[44] For higher voltages ($eV \leqslant E_F$) the exact calculation of Eq. (5) shows an overall decrease of the conductance which cannot be explained in terms of this simple approximation (Ref. 21). However, for the voltages discussed in this work, there are no noticeable differences between exact and approximate results.
[45] M. Büttiker, Phys. Rev. B **41**, 7906 (1990).
[46] A. G. Scherbakov, E. N. Bogachek, and U. Landman, Phys. Rev. B **53**, 4054 (1996).
[47] J. A. Torres, J. I. Pascual, and J. J. Sáenz, Phys. Rev. B **49**, 16 581 (1994).
[48] P. García-Mochales and P. A. Serena, Phys. Rev. Lett. **79**, 2316 (1997).
[49] E. Bascones, G. Gómez-Santos, and J. J. Sáenz, Phys. Rev. B **57**, 2541 (1998).
[50] A theoretical description of a conductance histogram should involve a detailed molecular dynamics calculation of the nanocontact evolution during many breakage processes, and a nontrivial evolution of transmission coefficients in a fully 3D problem. Additional effort should be done repeating this computational scheme for several bias voltages. Therefore an accurate description of conductance histograms may require an enormous effort out of the scope of the present work.
[51] Experimental shapes of gold contacts obtained in a high-resolution transmission electron microscope [T. Kizuka, K. Yamada, S. Deguchi, M. Naruse, and N. Tanaka, Phys. Rev. B **55**, R7398 (1997); H. Ohnishi, Y. Kondo, and K. Takayanagi, Nature (London) **395**, 780 (1998)] show a time evolution path at almost constant θ. It would be extremelly interesting to check the predicted nonlinear behavior (cf. Fig. 2) under this atomic-scale controlled situation.
[52] M. Zagoskin, Phys. Rev. B **58**, 15 827 (1998).
[53] T. N. Todorov, J. Hoekstra, and A. P. Sutton, Philos. Mag. B **80**, 421 (2000).
[54] It is worth noticing that the concept of effective elongation path reflects a sort of ensemble average between different ''static'' realizations. This average does not destroy the underlying conductance quantization effects. This is in contrast with conductance values (time) averaged over different contact cross sections which certainly must lead to the disappearance of quantized peaks.